Pathfinder Sea Surface Temperature Algorithm

Version 4.0 *(February 6, 1998)*

Robert Evans and Guillermo Podestá

University of Miami
Rosenstiel School of Marine and Atmospheric Science

Recent Updates and Changes

Table of Contents

Foreword

This document describes the algorithm used to compute sea surface temperature (SST) values in the AVHRR Pathfinder Oceans global SST products, Version 4.0.

Introduction

The need for accurate global sea surface temperature fields has been receiving increasing attention, primarily due to its importance in understanding variability in the oceans' climate. Satellite SST measurements are attractive due to their global, repeated coverage, compared to any other type of measurements. Since 1981, the NOAA series of polar-orbiting spacecraft have carried the Advanced Very High Resolution Radiometer (AVHRR), an instrument with three infrared (IR) channels suitable for estimating SST [Schwalb, 1978]. These channels are located in the wavelength regions between 3.5µm and 4µm and between 10µm and 12.5µm, where the atmosphere is comparatively transparent.

At IR wavelengths, the ocean surface emits radiation almost as a blackbody. In principle, without an absorbing and emitting atmosphere between the sea surface and the satellite, it would be possible to estimate SST using a single channel

measurement. In reality, surface-leaving infrared radiance is attenuated by the atmosphere before it reaches a satellite sensor. Therefore, it is necessary to make corrections for atmospheric effects. Water vapor, CO_2, CH_4, NO_2 and aerosols are the major constituents that determine the atmospheric extinction of IR radiance [Minnett, 1990]. Among them, absorption due to water vapor accounts for most of the needed correction [Barton *et al.*, 1989].

Various techniques have been proposed to account for the atmospheric absorption of surface IR radiance, and to produce accurate retrievals of SST. Anding and Kauth [1970] found that the difference in measurements at two properly selected infrared channels is proportional to the amount of atmospheric correction required. Using differences in brightness temperatures measured by an early satellite radiometer, Prabhakara *et al.* [1974] estimated SST to a reasonable accuracy. In a recent review of techniques to derive SST from satellite IR measurements, Barton [1995] shows that the differential absorption is exploited in all IR SST algorithms, and that there is a basic form for most algorithms:

$$SST = aT_i + gamma\ (T_i - T_j) + c$$

where T_i and T_j are brightness temperature measurements in channels i and j, and a and c are constants. The gamma term is defined as

$$gamma = (1 - t_i) / (t_i - t_j),$$

where t is the transmittance through the atmosphere from the surface to the satellite. In cases of weak absorption, the transmittance can be approximated by (1 - *ku*), where *k* is the mass absorption ccoefficient of the atmospheric absorbers and *u* is the path length [Barton, 1995].

All AVHRR algorithms share the general form described above, although various modifications have been introduced through the years to improve performance. McClain *et al.* [1985] developed algorithms for SST retrieval based on linear differences in brightness temperatures among AVHRR channels. This so-called MCSST algorithm assumed a constant gamma. The MCSST algorithm was NOAA's operational procedure for several years [McClain et al., 1985]. Subsequent improvements incorporated a correction for increased path lengths at larger satellite zenith angles [Cornillon et al., 1987]. Other improvements in the atmospheric correction involved nonlinear formulations, in which gamma was proportional to the brightness temperatures, as in the CPSST (cross-product SST) algorithm described by Walton [1988] and Walton et al. [1990].

The latest version of the operational NOAA algorithm is the NLSST (non-linear SST), in which gamma is assumed to be proportional to a first-guess SST value (which can be obtained in various ways). The AVHRR Oceans Pathfinder SST algorithm (which is used to produce the Pathfinder SST or PFSST global fields) is based on the NLSST algorithm developed by C.Walton [Walton et al. 1998]. The NLSST algorithm has the following form:

$$SST_{sat} = a + b\ T_4 + c\ (T_4 - T_5)\ SST_{guess} + d\ (T_4 - T_5)\ (sec(rho) - 1),$$

where SST_{sat} is the satellite-derived SST estimate, T_4 and T_5 are brightness temperatures in AVHRR channels 4 and 5 respectively, SST_{guess} is a first-guess SST value, and rho is the satellite zenith angle. Coefficients a, b, c, and d are estimated from regression analyses using co-located in situ and satellite measurements (or "matchups"). Typically, NOAA produced a set of coefficients using matchups for a certain period; these coefficients would not be modified until there was a perceived need (e.g., after the eruption of the Mt. Pinatubo volcano in June 1991, or when a new AVHRR was launched).

The Pathfinder Match-up Database

SST algorithm coefficients based on IR measurements can be estimated in two major ways. The first alternative involves the use of a radiative transfer model and a set of atmospheric vertical profiles (temperature, humidity), which are used to simulate at-satellite brightness temperatures (BTs). The simulated BTs are subsequently regressed against *in situ* SST measurements in order to derive algorithm coefficients. This semi-physical approach has been adopted to develop algorithms for the Along-Track Scanning Radiometer (ATSR) onboard the ERS-1 satellite. It must be noted that this approach produces so-called "skin temperature" estimates (the skin is the uppermost layer of the ocean, responsible for the IR emission). The skin temperature may differ from the "bulk" temperature usually measured by traditional *in situ* instruments (e.g., buoys).

A second alternative for estimating SST algorithm coefficients is a regression between *in situ* SST measurements and nearly-coincident satellite observations (matchups). This produces a statistical algorithm, tuned to bulk SST measurements. Differences between skin and bulk SST algorithms are discussed by Wick et al. [1992]. The statistical approach has been followed for the estimation of coefficients for the Pathfinder SST (PFSST) algorithm.

One highlight of the AVHRR Pathfinder Oceans program is that, for the first time, a set of coincident *in situ* and satellite measurements, used for algorithm development and testing, is being distributed together with the global SST products. A

complete description of the Pathfinder Matchup Database (PFMDB), including information on how to obtainthe matchup files, can be found in http://www.rsmas.miami.edu/groups/rrsl/pathfinder/match_index.html. For the purpose of algorithm estimation, there are two relevant points regarding the matchups. First, the Pathfinder matchups have tight space-time constraints: *in situ* and satellite observations are deemed coincident if they occur within ±30minutes and ±0.1° of latitude and longitude of one another. Second, the PFMDB has been screened carefully to identify *most* cloud-contaminated matchups, so they could be excluded from the coefficient estimation stage. Subsequently, any discussion of matchups in the context of algorithm estimation and testing will imply the use of cloud-screened matchups, unless otherwise indicated.

The Pathfinder SST Algorithm

The NLSST formulation developed by C. Walton (formerly at NOAA/NESDIS) and described in Walton et al. [1998] was adopted as the basis for the AVHRR Oceans Pathfinder SST algorithm (PFSST) because of its adequate performance and its operational nature in NOAA products. Nevertheless, a few minor modifications were introduced to NOAA's NLSST; these modifications are described in the following paragraphs.

Separate coefficients for two (T_4 - T_5) regimes

Various diagnostics performed on residuals (defined as observed minus predicted SSTs, or *in situ* minus satellite SSTs) from earlier versions of the Pathfinder SST algorithm suggested that the association between the ($T_4 - T_5$) values (hereafter referred to as T45) and the bias of the atmospheric correction was somewhat different for dry and moist atmospheres. For instance, there seemed to be a consistent positive bias in SST residuals at low T45 values; this was true for all satellite zenith angle values. Also, we attempted to find optimal empirical transformations to linearize associations between predictand and predictor variables prior to regression. The estimated empirical transformations showed a change in their shape at T45 values around 0.7–1.0°C. This suggests a change in the underlying functional form of the association between T45 and SST. A full discussion of the possible physical reasons behind this change is beyond the scope of this document. Nevertheless, it is likely that the balance between various sources of radiance sensed by the AVHRR instrument (e.g., radiance emitted by the ocean surface vs. atmospheric radiance) changes as a function of atmospheric moisture. Furthermore, the effects of ocean surface emissivity, air-sea temperature differences, and atmospheric absorbers other than water vapor become more relevant in drier atmospheres.

As an empirical approach to capturing the change in the nature of the functional association between AVHRR radiances and SST, we implemented a piece-wise fit to algorithm coefficients. Algorithm coefficients were estimated separately for (a) low, and (b) intermediate to high T45 values. The chosen boundary between the two regimes was T45=0.7°C. To avoid discontinuities in the global PFSST fields as the computation switches from one set of coefficients to another, we implemented a transition in the SST calculation, which is described in detail below.

Coefficients estimated for monthly periods

Earlier versions of the PFSST algorithm had been estimated with a single set of coefficients per T45 regime for the entire span of an AVHRR's lifetime. Initial diagnostics, however, suggested the presence of temporal trends in the algorithm performance. The trends included a variety of temporal scales, from seasonal (e.g., higher bias and rms in SST esiduals during Northern Hemisphere summers) to interannual. The interannual trend was of unclear origin and could be due to changes in the radiometric sensitivity of an AVHRR as it ages, or changes in the operating conditions. For instance, during the later stages of NOAA-9 and NOAA-11's operational lifetimes, the baseplate on which the onboard calibration targets are mounted was operated at a significantly higher temperature than during previous years (also, at higher temperatures than those used for pre-launch sensor characterization).

To reduce the presence of trends in the SST estimates, the PFSST coefficients were estimated on a month by month basis. We used a window of five months of matchups centered on the month for which coefficients were being estimated. Matchups for each period in the window were weighted differently: the central month (e.g., month N) was assigned a weight of 1.0, for adjacent months (N – 1 and N + 1) the weights were 0.8, and weights of 0.5 were used for the ends of the 5-month window (months N – 2 and N + 2). In selecting these weights, no attempt was made to reflect the statistical structure (*i.e.,* temporal correlation) of the SST values. Instead, the main goal was to ensure greater statistical weight for the matchups from the central month. Also, note that the weights do not add up to 1.0, as they are intended to convey an idea of the relative temporal weighting. The weights are normalized so they add up to 1.0 during the weighted regression procedure.

The weighting scheme for the ends of the data series for a given instrument was defined differently. For the first and last months of an AVHRR series, we used a 3-month window, and for the second and next-to-last months we used a 4-month window. The matchup windows used for each month in a series, together with their respective weights, are illustrated in Figure 1. In all cases, the temporal weights were subsequently combined with robustness weights derived from residuals from a first-estimate of SST values; more on this below. Growing data sets are an eception; this is discussed below.

For the Pathfinder algorithms estimated to date, there are three major exceptions to the scheme described in Figure 1. First, the NOAA-11 data set was treated as two separate series, with the separation corresponding to the main eruption of Mt. Pinatubo (approximately, June 15, 1991). This implies that (a) two sets of coefficients were estimated for June 1991 corresponding to pre- and post-Pinatubo conditions, and (b) the first and second halves of June 1991 were treated, respectively, as the end and the beginning of two series (the weighting schemes described above for the ends of a series were used).

The second exception was the NOAA-9 data used to fill the gap (September 1994–January 1995) between the demise of NOAA-11 and the beginning of the NOAA-14 operational period. Because of the short span of this data series, a single set of algorithm coefficients was estimated for each T45 regime for the entire NOAA-9 gap, without using temporal weighting. For the beginning of NOAA-14, the first period (nominally labelled February 1995) included a few days of January 1995.

The third exception to the weighting scheme described above corresponds to growing data sets (e.g., NOAA-14). , matchups are usually developed one year at a time. The algorithm coefficients also are estimated for that year once matchups are released. The three months at the end of each year in a growing data set (e.g., October, November and December 1998) are estimated without matchups for the following year. For example, coefficients for November 1998 should be estimated using matchups from September 1998 to January 1999. If the 1999 matchups are unavailable, coefficients are estimated using matchups from September to December 1998. In this case weights are the reverse of what is shown in Figure 1b. Theoretically, once 1999 matchups become available, the coefficients for the last three months of 1998 could be re-estimated. In order to provide coefficients as soon as possible and avoid having to reprocess porducts, we have decided NOT to revise coefficients for the end of a growing data set. The result is that the last three months of a year will be estimated with less than five months of matchups.

Figure 1. Temporal window used in the estimation of PFSST algorithm coefficients for a given month or period. The figure illustrates the number of months used and the weights asigned to matchups for each month for (a) the first month in a series, (b) the second month in a series, and (c) months in the middle of a series. For data at the end of a series, the coefficients are estimated using the mirror images of cases (a) and (b). The dark bar indicates the month (or period) for which coefficients are estimated.

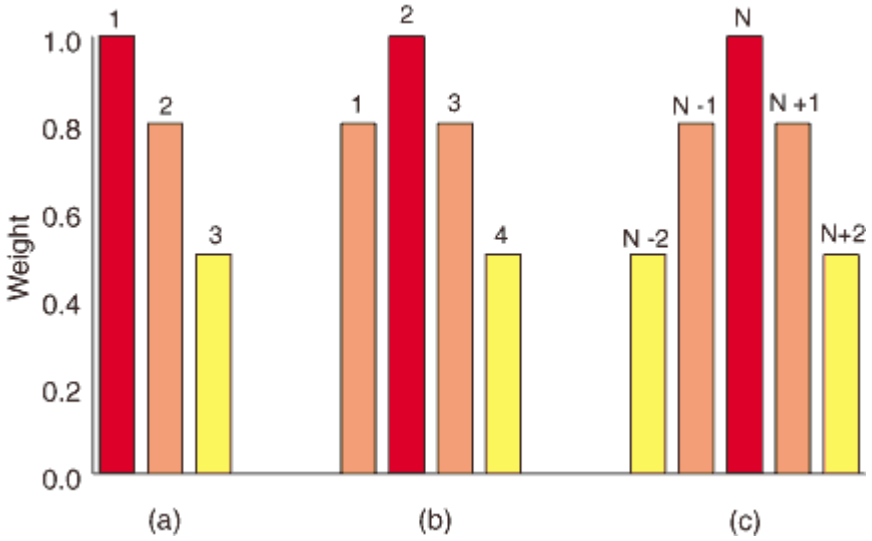

Algorithm Coefficient Estimation

Before matchups are used for coeficient estimation, one needs to exclude those records likely to be cloud-covered or cloud-contaminated. Other factors (e.g., AVHRR digitization errors) may introduce errors in the satellite measurements as well. Several methods have been proposed in the literature to identify cloud-covered pixels in AVHRR imagery; a few examples include the work of Saunders and Kriebel [1988], Derrien et al. [1993], Luo et al. [1995] and Cayula and Cornillon [1996]. The procedures used to identify cloud contamination and other potentially erroneous satellite measurements in the Pathfinder matchups are described in detail in the Pathfinder Matchup Database documentation. Briefly, the matchups cloud and outlier flagging involves a series of tests based on thresholds of differences between brightness temperatures in two different channels, and spatial homogeneity tests.

Despite the cloud-flagging tests, there are always a few matchups that lead to large SST residuals (i.e., large differences between observed and estimated SSTs). This maybe due to a failure of the cloud tests, or also to problems with the *in situ* values (e.g., a miscalibrated buoy). Outliers (matchups with high SST residuals) can unduly influence coefficient estimates, so they need to be excluded from the estimation procedure. In an earlier version of the algorithm estimation, we had excluded

matchups with absolute value of residuals>2°C (with respect to a first guess SST). Given the relatively good performance of the cloud flagging tests, very few extreme values were excluded by the ±2°C test, and thus this test should not have influenced significantly our earlier asessments of algorithm performance (despite the fact that a threshold was used to exclude large residuals). Nevertheless, we explored other alternatives that would not involve a fixed threshold for exclusion of matchups leading to high SST residuals. Such a procedure was implemented in Version 4.0 of the Pathfinder products.

Additional tests. Two additional tests were implemented for selection of matchups to be used in the processing of NOAA-14 data for 1998 and 1999. These tests were as follows:

- (T4 - T5) >= 0 deg C: In a few cases, the difference between brightness temnperatures in AVHRR channels 4 and 5 was negative (indicating that T5 > T4). This may suggest an error in the measurements or anomalous atmospheric conditions under which the algorithms are not likely to yield good SST retrievals. For that reason, matchups for which (T4 - T5) < 0 deg C were excluded. This test was used for NOAA-14 matchups starting in 1998.
- T4 >= 2.5 deg C. We discovered a problem with the NOAA-14 digitizer that caused problems in T4 values lower than about 2.5 deg C (the location changes slightly with time). We excluded all matchups for which T4 < 2.5 deg C. This test was applied to NOAA-14 matchups starting with 1999. A more detailed description of the NOAA-14 digitizer problem can be found here.

In the current Pathfinder protocol, algorithm coefficient estimation is a three-stage process. In the first stage, those matchups which passed the cloud and outlier flagging tests (see description of Pathfinder matchups) and some additional tests are used to estimate a first-guess set of coefficients using a resistant regression procedure, in which coefficient estimates are relatively insensitive to large outliers. The first-guess coefficients are used to compute first-guess SST residuals. In a second stage, the first-guess residuals are used to compute robustness weights, to decrease the influence of large residuals in the final coefficient estimation. In the third and last stage, robustness weights and temporal weights are used in a weighted least squares regression. That is, matchups with large first-guess residuals have a lower weight in the final coefficient estimation. The third stage produces the operational set of coefficients. This procedure is repeated for each period for which coefficients are estimated (usually, a month), and for each T45 regime. We discuss each of the three stages in more detail below.

Estimation of First-guess SST Residuals

All matchups that passed the cloud-flagging and additional tests were used to estimate a first-guess set of algorithm coefficients. Because cloud-contaminated matchups may remain after cloud-flagging tests, we used a modern resistant regression procedure, in which large outliers do not unduly influence the first-guess coefficient values. For all satellites up to NOAA-14 1997 data, we used a procedure called Least Trimmed Squares or LTS [Rousseeuw and Leroy, 1987], which returns a regression estimate that minimizes the sum of the smallest half of the squared residuals. The LTS method has a very high breakdown point. In statistical terms, the breakdown point indicates the proportion of outliers that can be present in a data set before estimates are strongly influenced; the higher the breakdown point, the more resistant the procedure [Lanzante, 1996]. The resistant regression was repeated for each T45 regime and for each period for which algorithm coefficients were estimated.

Starting with NOAA-14 data for 1998, the robust regression procedure used changed. Instead of the LTS procedure, we adopted a new procedure called robust MM regression. The theory for this method is based on Rousseeuw and Yohai [1984], Yohai, Stahel and Zamara [1991], and Yohai and Zamar [1998]. The procedure we used was implemented in the commercial software package S-Plus as function `lmRobMM()`.

The first-guess algorithm coefficients were used to compute first-guess SST residuals (*in situ* SST minus first-guess SST). These first-guess residuals were then used to derive obustness weights used as input to a subsequent stage of coefficient estimation. The goal was to assign reduced weights to large first-guess residuals (for instance, those due to unidentified cloud contamination) in order to reduce their influence on subsequent coefficient estimation.

Computation of Robustness Weights

To derive robustness weights from the first-guess SST residuals, we followed a sequence of steps. First, we estimated, for each period and T45 regime, the median of the absolute values of first-guess residuals; this quantity is designated MAD, which stands for median absolute of deviations. Second, we used the bisquare function to compute robustness weights. The bisquare function B*(u)* , where *u* denotes the function's argument, has a value of $(1 - u^2)^2$ for $| u | < 1$, otherwise it is zero. The first-guess residuals (denoted as e), their corresponding MAD (for a given period and T45 regime), and the bisquare function B were used to compute robustness weights r as

$$r = B [e / (6 * MAD)] .$$

The previous equation indicates that the robustness weights have a value of zero for matchups with first-guess residuals greater than ±6 * MAD. The factor of 6 multiplying the MAD was selected so that, if the first-guess residuals have an underlying Gaussian distribution, this threshold is approximately equivalent to rejecting first-guess residuals beyond ±4 standard deviations. In most cases, MAD values ranged betwen 0.3° and 0.4°C: this implies that residuals with absolute values greater than 1.8° to 2.4°C were excluded (i.e., had weights equal to zero). Robustness weights are illustrated in Figure 2.

Figure 2. Robustness weights computed using the bisquare function and MAD values of 0.3°C (solid line) and 0.4°C (dashed line). See text for explanation.

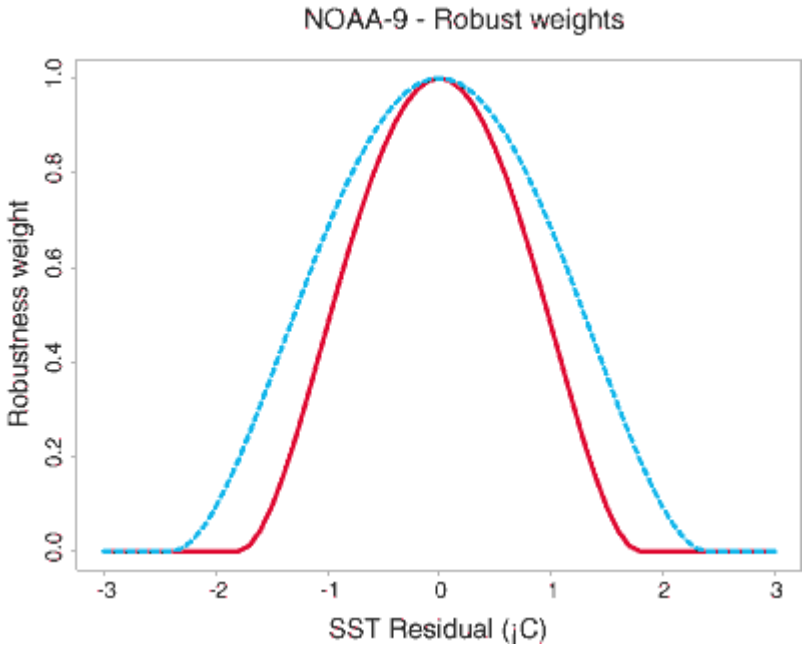

Weighted Least-squares Estimation

The last stage of the coefficient estimation procedure involves a weighted least squares procedure. The robustness weights derived in the previous stage were multiplied by the temporal weights (see "Coefficients estimated for monthly periods"), and the resulting values were the final weights used as input to a weighted least squares regression. The weight assigned to a particular matchup for coefficient estimation, therefore, was a function of (a) its first-guess SST residual, and (b) its temporal separation from the month for which coefficients were being estimated. The coefficients estimated by the weighted least squares regression were used to process the global Pathfinder SST fields. The coefficients for each AVHRR, month, and T45 regime are shown in the Appendix to this document.

What is the advantage of using the approach described in previous paragraphs? In earlier versions, the PFSST coefficients showed temporal fluctuations at scales of months to years. Although fluctuations in the coefficient for one term of the algorithm usually were compensated somewhat by the values of coefficients for other terms, it was unclear if this had consequences on algorithm performance. To assess the advantages of the resistant procedure, we first estimated a set of coefficients using unweighted least squares on the matchups that passed the cloud-flagging tests (Procedure A). A second set of coefficients (Procedure B) was estimated by imposing a ±2°C limit on SST residuals derived from Procedure A, and re-estimating coefficients (using unweighted least squares) excluding residuals higher than that limit. Finally, we performed the coefficient estimation using the resistant regression followed by weighted least squares, as described in previous paragraphs (Procedure C).

Figure 3 shows the values of the first two algorithm coefficients (the constant term and the term multiplying T4) in the PFSST algorithm for NOAA-9 matchups. The three lines correspond to coefficients estimated following Procedures A, B and C, as described above. It is clear that the temporal stability of the coefficients is much greater, and this is conceptually attractive. These results may make one consider whether separate monthly coefficients are necessary. Although the resistant regression estimation seems to reduce considerably seasonal fluctuations in the coefficients, they have not disappeared entirely. Furthermore, still there are unexplained low-frequency trends in coefficient values. Therefore, for the current version of the Pathfinder fields we still use monthly coefficients.

Figure 3. Time series of the first two algorithm coefficients for NOAA-9, 1985–1988. Coefficient 1 is the constant term, and Coefficient 2 is the T4 multiplier. The coefficients correspond to matchups with T45 values > 0.7°C. The open circles indicate coefficient values estimated using unweighted least squares regression on all matchups that passed the cloud flagging tests

(Procedure A in text). The asterisks denote coefficients estimated by (i) using straight least squares as described in previous sentence, (ii) excluding residuals with absolute values greater than 2.2°C, and (iii) reestimating coefficients using straight least squares (Procedure B in text). The solid circles indicate coefficient values estimated via a resistant regression, followed by a weighted least squares regression (Procedure C in text).

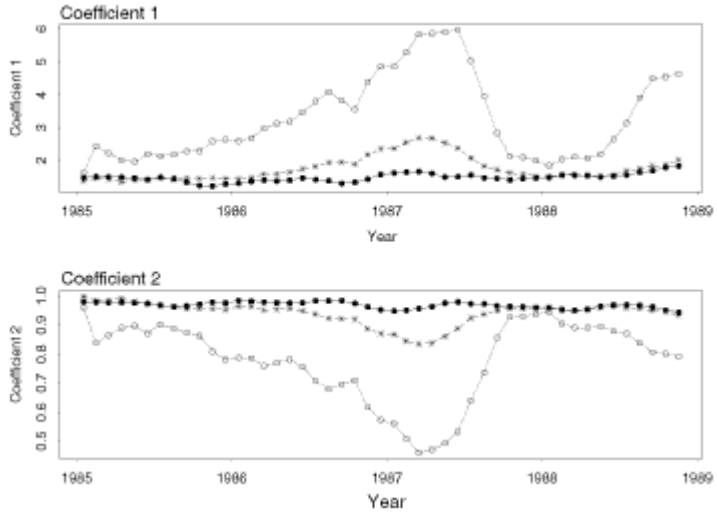

SST Computation at T45 Regime Transition

The separate estimation of coefficients for two T45 regimes (above and below T45 = 0.7°C) could result in discontinuities in the global PFSST fields as the computation switches from one set of coefficients to another. To avoid these effects, we implemented a transition in the calculation which was used in the processing of the Pathfinder SST fields. To assess algorithm performance using the matchups, the transitional calculation was used for the matchups.

Basically, the procedure involves the computation of two intermediate PFSSTs for each matchup, respectively using coefficients corresponding to either T45 regime in the period. The final PFSST is computed as the weighted sum of the two intermediate SSTs, where the weight is a function of the T45 value. That is,

$$PFSST = w1 * PFSST1 + (1 - w1) * PFSST2$$

where PFSST is the Pathfinder SST, PFSST1 and PFSST2 are the SSTs computed using the algorithm coefficients for low and high T45 regimes, respectively, and w1 is a weighting factor which varies as a function of T45 as follows:

- For T45 <= 0.5°C, w1 = 1.0
- For 0.5°C < T45 < 0.9°C, w1 = 1 - ((T45 - 0.5°) / (0.9° - 0.5°))
- For T45 >= 0.9°C, w1 = 0.0

That is, for T45 <= 0.5°C, the PFSST is computed using only the coefficients for low T45 regimes. Similarly, for T45 >= 0.9°C, only the coefficients for high T45 regimes are used. For T45 values between 0.5°C and 0.9° (i.e., a ±0.2° interval around the 0.7°C boundary between T45 regimes), the final SST is a linear combination of the SSTs computed from both sets of coefficients.

Algorithm Coefficients – Pathfinder SST Fields Version 4

The algorithm coefficients estimated in the manner described above, and used to compute the AVHRR Ocean Pathfinder global SST fields denoted as Version4 are listed in a separate file [Click here to link to the coefficients' file].

Algorithm performance

A detailed characterization of algorithm performance is beyond the scope of this document. However, to give potential users of the Pathfinder SST fields a feel for the variability in SST estimates, we provide boxplots of SST residuals (*in situ* SST minus

Pathfinder SST) for the AVHRRs operating during the period 1985–1995 (Figure 4). For each operational AVHRR, boxplots are shown for four latitudinal bands: 40°–20°S, 20°S–20°N, 20°–40°N, and 40°–60°N. No results are shown for latitudes below 40°S or above 60°N due to the paucity of matchups in those regions.

In most cases, each box and whiskers in a panel corresponds to a month. Exceptions include the June 1991 period for NOAA-11, separated into pre- and post-Pinatubo (Figure 4b). The first month of NOAA-14 includes data only for a few days of January 1995 (Figure 4c).For each period, the dot represents the median of SST residuals in a period and the box encompasses the central 50% of the residuals (i.e., data between the 25-percentile and the 75-percentile). The whiskers indicate residuals within 1.5 times the width of the box. Individual dashes are extreme outliers (beyond the whiskers' length). The dashed vertical lines in each panel indicate -0.2°, 0° and 0.2°C. In general, each box and whiskers (corresponding to a given month and latitudinal band) contains at least 100 matchups, therefore statistics are considered stable.

One important feature is the bias introduced by aerosols from the Mt. Pinatubo main eruption (June 1991). This is particularly noticeable in the tropical latitudes, and it takes several months for residuals to approach normal. Another important point is that, in general, the tropical band shows a negative bias of about 0.1°–0.2°C, that is, SST algorithms are under-correcting. In contrast, the band between 20°N and 40°N, where most matchups occur, tends to show a positive bias (over-correcting). It is remarkable that the central half of the residuals (denoted by the boxes) shows a fairly tight distribution.

We stress that the residuals used to produce Figure 4 were computed using the actual *in situ* SST as the first-guess value in the algorithm. In contrast, the first-guess SST in the Pathfinder field calculations was the Reynolds Optimally Interpolated SST (see document on Pathfinder Matchups for description). The SST residuals computed using the values on the global fields, then, can be slightly different.

Figure 4a. Boxplots of Pathfinder SST residuals for NOAA-9, January 1985 to November 1988. See text for description of the plots.

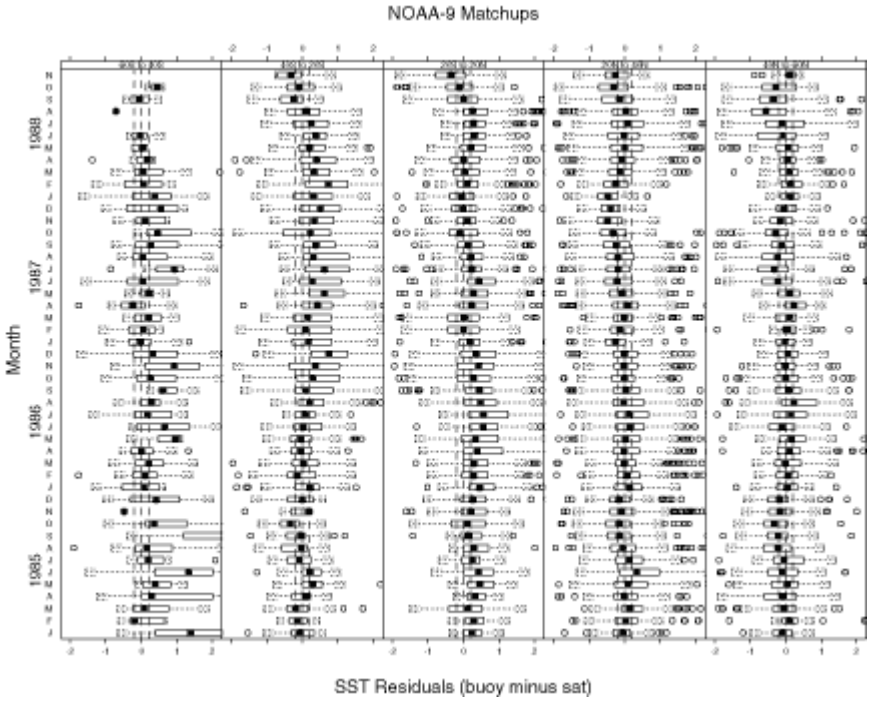

Figure 4b. Boxplots of Pathfinder SST residuals for NOAA-11, November 1988 to September 1994. See text for description of the plots.

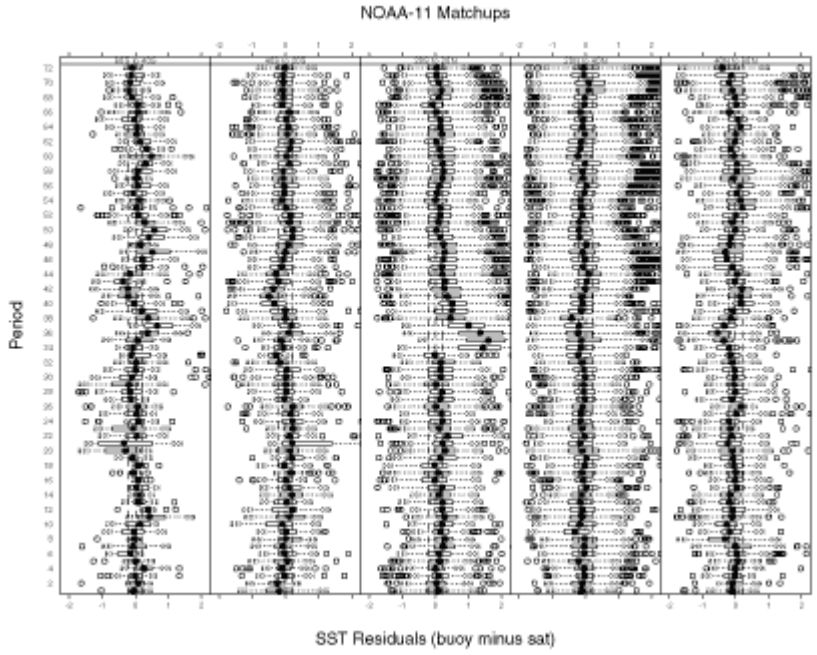

Figure 4c. Boxplots of Pathfinder SST residuals for NOAA-9 gap period, September 1994 to March 1995. See text for description of the plots.

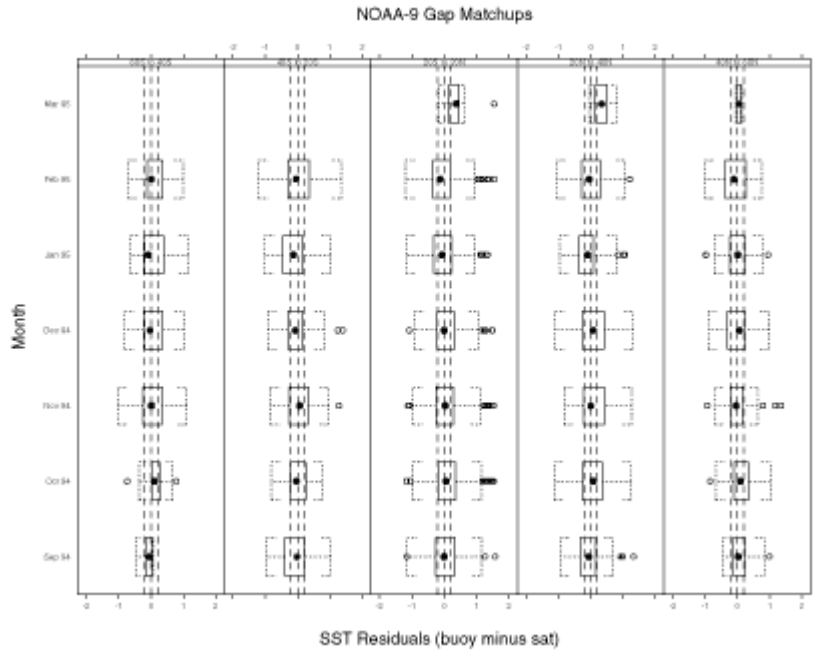

Figure 4d. Boxplots of Pathfinder SST residuals for NOAA-14, February 1995 to December 1999. See text for description of the plots.

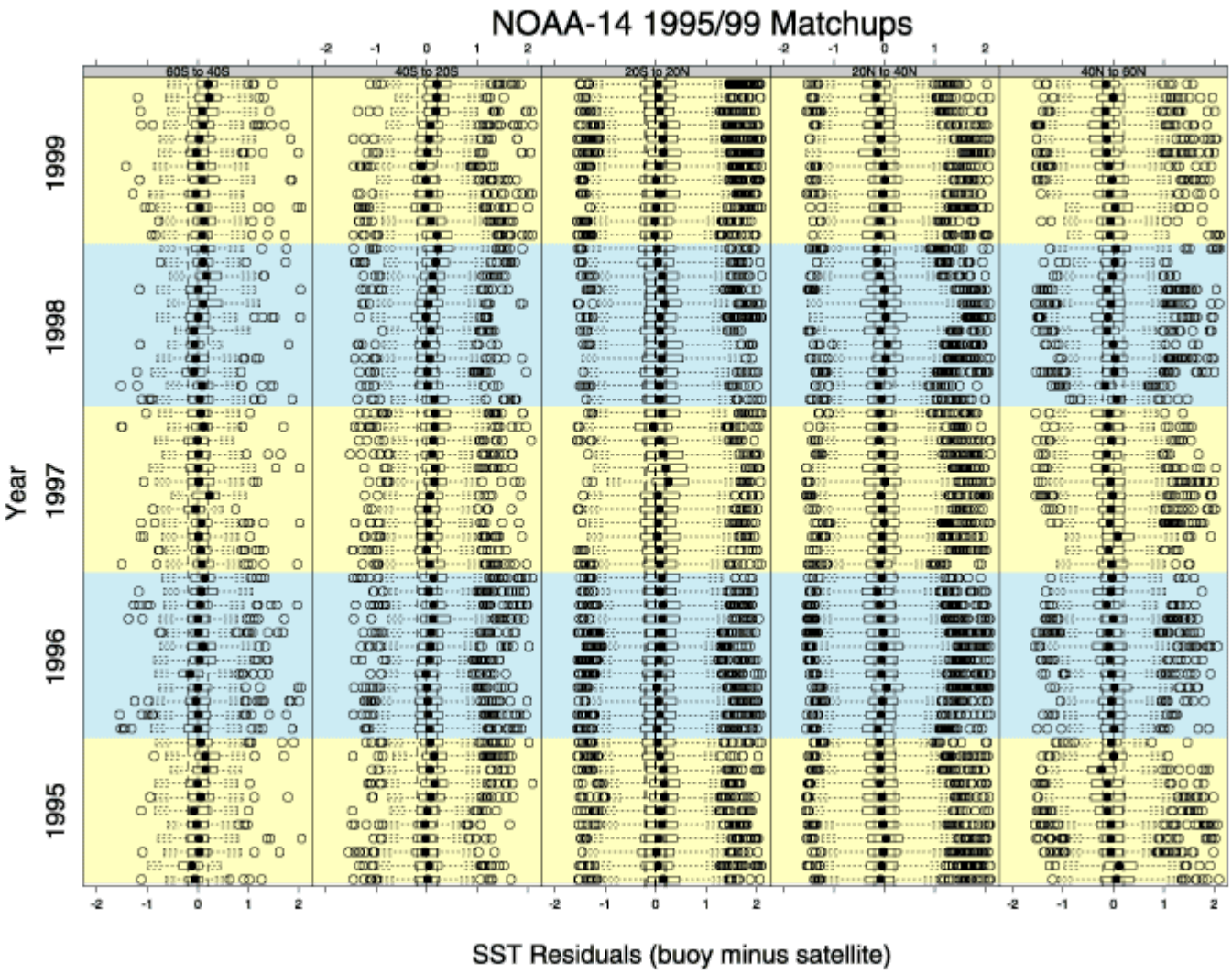

Global vs. Regional Algorithms

The main challenge in developing a Pathfinder global SST algorithm is to achieve relatively uniform performance throughout a wide range of atmospheric and oceanic conditions. As Barton [1995] pointed out, SST algorithms assume a first guess of the state of the atmosphere (e.g., a typical shape of water vapor and temperature profiles). A similar statement can be made about typical oceanic conditions (e.g., a certain average structure of the ocean's uppermost layer is assumed in comparisons with *in situ* SST measurements). When conditions deviate from the implicit first guess in atmosphere and ocean conditions, errors arise in SST retrievals. Deviations from implicit first-guess conditions are more likely in a global algorithm than in regionally-tuned algorithms, and this should be kept in mind when evaluating global SST estimates. Furthermore, in the case of statistically-derived global SST algorithms, the first-guess conditions will be the average of conditions at all the matchup locations and times used in coefficient estimation. We stress that this average will be weighted by the relative distribution of matchups, likely to change in time. The performance of an SST algorithm for a given set of atmospheric and oceanic conditions, therefore, depends not only on how close those conditions are to the average state, but also on how well represented are those conditions in the matchup set used to derived the algorithm coefficients.

References

Anding, D, and R. Kauth. 1970. Estimation of sea surface temperature from space. Remote Sensing of the Environment 1: 217-220.

Barton, I.J., 1995. Satellite-derived sea surface temperatures: Current status. Journal of Geophysical Research 100: 8777–8790.

Barton, I.J. and R.P. Cechet. 1989. Comparison and optimization of AVHRR sea surface temperature algorithms. Journal of Atmospheric and Oceanic Technology 6: 1083–1089.

Cayula, J.-F. and P. Cornillon. 1996. Cloud detection from a sequence of SST images. Remote Sensing of the Environment 55: 80–88.

Cornillon, P., C. Gilman, C., L. Stramma, O. Brown, R. Evans and J. Brown. 1987. Processing and analysis of large volumes of satellite-derived thermal infrared data. Journal of Geophysical Research 92: 12,993–13,002.

Derrien, M., B. Farki, L. Harang, H. LeGléau, A. Noyalet, D. Pochic and A. Sairouni. Automatic cloud detection applied to NOAA-11/AVHRR imagery. Remote Sensing of the Environment 46: 246–267.

Emery, W.J., Y. Yu, G.A. Wick, P. Schluessel and R.W. Reynolds. 1994. Correcting infrared satellite estimates of sea surface temperature for atmospheric water vapor contamination. Journal of Geophysical Research 99: 5219–5236.

Lanzante, J.R. 1996. Resistant, robust and non-parametric techniques for the analysis of climate data: Theory and examples, including applications to historical radiosonde station data. International Journal of Climatology 16: 1197–1226.

Luo, G., P.A. Davis, L.B. Stowe and E.P. McClain. 1995. A pixel-scale algorithm of cloud type, layer and amount for AVHRR data. Part I: Nightime. Journal of Atmospheric and Oceanic Technology 12: 1013–1037.

McClain, E.P., W.G. Pichel and C.C. Walton. 1985. Comparative performance of AVHRR-based multichannel sea surface temperatures. Journal of Geophysical Research 90: 11,587–11,601.

Minnett, P.J. 1990. The regional optimisation of infrared measurements of sea surface temperature from space. Journal of Geophysical Research 95: 13,497–13,510.

Prabhakara, C., G. Dalu and V.G. Kunde. 1974. Estimation of sea surface temperature from remote sensing in the 11 to 13-um window region. Journal of Geophysical research 79: 5039-5044.

Rousseeuw, P.J. and A.M. Leroy. 1987. Robust regression and outlier detection. John Wiley & Sons. New York. 329 p.

Rousseeuw, P.J. and V. Yohai. 1984. Robust regression by means of S-estimators. In: *Robust and Nonlinear Time Series Analysis*, J. Franke, W. Hardle, and R.D. Martin (eds.), Lecture Notes in Statistics, 26, 256-272, Springer-Verlag.

Saunders, R.W. and K.T. Kriebel. 1988. An improved method for detecting clear sky and cloudy radiances from AVHRR data. International Journal of Remote Sensing 9: 123–150.

Schwalb, A. 1978. The TIROS-N/NOAA A-G satellite series. NOAA Technical Memorandum NESS 95. U.S. Government Printing Office. Washington, DC. 75 p.

Walton, C.C. 1988. Nonlinear multichannel algorithm for estimating sea surface temperature with AVHRR satellite data. Journal of Applied Meteorology 27: 115–124.

Walton, C.C., E.P. McClain and J.F. Sapper. 1990. Recent changes in satellite based multichannel sea surface temperature algorithms. Marine Technology Society Meeting, MTS' 90, Washington D.C, September 1990.

Walton, C. C., W. G. Pichel, F. J. Sapper, and D. A. May, 1998. The development and operational application of nonlinear algorithms for the measurement of sea surface temperatures with NOAA polar-orbiting environmental satellites. Journal of Geophysical Research 103: 27999–28012.

Wick, G.A., W.J. Emery and P. Schluessel. 1992. A comprehensive comparison between satellite-measured skin and multichannel sea surface temperature. Journal of Geophysical Research 97: 5569–5595.

Yohai, V., W.A. Stahel, and R.H. Zamar. 1991. A procedure for robust estimation and inference in linear regression. In: *Directions in Robust Statistics and Diagnostics, Part II,* Stahel, W.A., and S.W. Wesiberg (eds.), Springer-Verlag, New York.

Yohai, V., and R.H. Zamar. 1998. Optimal locally robust M-estimates of regression. J. of Statist. Inf. and Planning.

Appendix A. List of algorithm coefficients.

Coefficient values for the various AVHRRs are listed in Appendix A. Click on the appropriate line below to view the appropriate coefficients.

- NOAA-7 (currently unavailable)
- NOAA-9 main data sequence
- NOAA-11
- NOAA-9 gap
- NOAA-14 (1995-1999 available)

| MAIN HOME PAGE |

Page last Updated: Saturday, June 30, 2001 at 6:54 PM

Contact: Guillermo Podestá (gpodesta@rsmas.miami.edu), Telephone:+1.305.361.4142